ELECTRONIC PROPERTIES OF CONDUCTING SYSTEMS

Electric properties of erbium cobaltites

Yu. N. Chiang[a] and M. O. Dzyuba

B. I. Verkin Institute for Low-Temperature Physics and Engineering of the National Academy of Sciences of Ukraine, pr. Lenina 47, Kharkov 61103, Ukraine

V. F. Khirnyĭ

Institute of Single Crystals and Scientific-Technological Concern "Institute of Single Crystals" of the National Academy of Sciences of Ukraine, pr. Lenina 60, Kharkov 61072, Ukraine

O. G. Shevchenko

B. I. Verkin Institute for Low-Temperature Physics and Engineering of the National Academy of Sciences of Ukraine, pr. Lenina 47, Kharkov 61103, Ukraine

A. A. Kozlovskiĭ

Institute of Single Crystals and Scientific-Technological Concern "Institute of Single Crystals" of the National Academy of Sciences of Ukraine, pr. Lenina 60, Kharkov 61072, Ukraine

(Submitted May 14, 2009; revised May 29, 2009)
Fiz. Nizk. Temp. **35**, 1123–1132 (November 2009)

The temperature and electric, including magnetic-field, characteristics of ceramic samples $Er_{1-x}Sr_xCoO_{3-\delta}$ at temperatures ranging from room to liquid-helium temperatures and in magnetic fields to 4 kOe applied perpendicular to the direction of the transport current have been investigated. Current-induced nonlinear features of percolation transport which are characteristics for a metal-insulator transition have been observed for weak currents. Regular behavior such as a decrease of the breakdown field with increasing concentration of divalent Sr and ordering effects with decreasing temperature have been observed for the first time. An anomalous increase of the conductivity and a large magnetoresistance effect in narrow Er and Sr concentration ranges, narrower and shifted more in the direction of the metallic phase than in lanthanum manganites, has been observed. The special behavior of the conductivity and the magnetoresistance, including nonlinear effects, are explained from a unified point of view—magnetostructural phase transitions, induced by a corresponding dopant concentration, temperature, or magnetic field, as well as the presence of a spin-dependent contribution, associated with double-exchange of delocalized electrons between heterovalent cobalt ions, to the mechanism of electron correlation.
[doi:10.1063/1.3266918]

I. INTRODUCTION

Extensive investigations of a number of multicomponent perovskite systems synthesized on the basis of elements possessing appreciable, often strong, magnetism have led to the conclusion that the unusual electron properties of these systems, such as high-temperature superconductivity or colossal magnetoresistance, are due to competition between the electrostatic and exchange, spin-spin and spin-orbital, interactions correlating electronic states from localized to delocalized.[1–4] For this reason interest in studying the properties of compounds containing transition and rare-earth elements with partially filled *d* and *f* shells—sources of magnetic moments capable of becoming ordered into some type of magnetic structures depending on the character of the competition between the exchange interactions—remains unabated. Experiments have shown that the character of the interactions which is responsible for the radical change in, say, the conductivity of transition-metal oxides occurs only in a definite interval of concentrations of the magnetic dopants, which give the optimal conditions of correlation (optimal magnitude and sign of the exchange integral) of local ionic magnetic moments and spins of the delocalized conduction electrons.[1–5] It has been found that, specifically, such a stable configuration of the local ionic spins as "ferromagnetic" ordering is always accompanied by an elevated conductivity, which indicates the vital role that conduction electrons play in establishing such a magnetic structure, in contrast to antiferromagnetic and paramagnetic distributions of the magnetic moments, characterized by a reduced or almost absent conductivity.[6,7]

Perovskite compounds are synthesized in crystalline structures with two sublattices whose planes can differ by the character of the alternation of the ionic spins within the planes as well as from one plane to another in a series of parallel planes, depending on temperature and dopant concentration. Figure 1 gives for a perovskite structure with allotropic forms of simple cubic-type sublattices an idea of the two-lattice structure of transition-metal perovskites, one sublattice of which is formed by the rare-earth dopant ions and alkali-earth atoms partially replacing them.

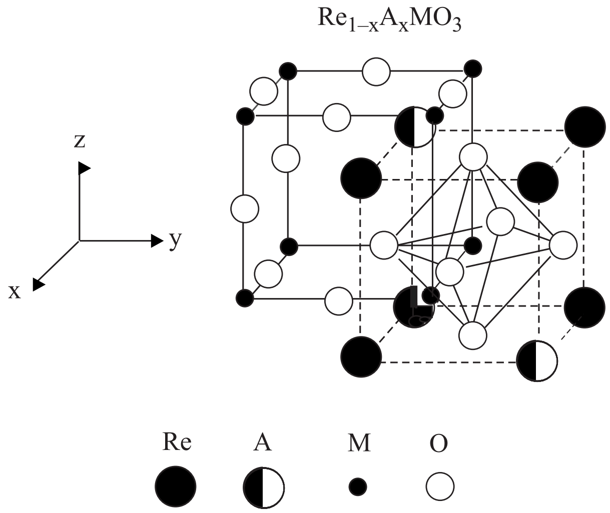

FIG. 1. Crystal structure with two cubic sublattices of certain perovskite compounds (R—*f*-magnet, A—nonmagnetic alkali-earth metal, M—*d*-magnet, O—oxygen atoms).

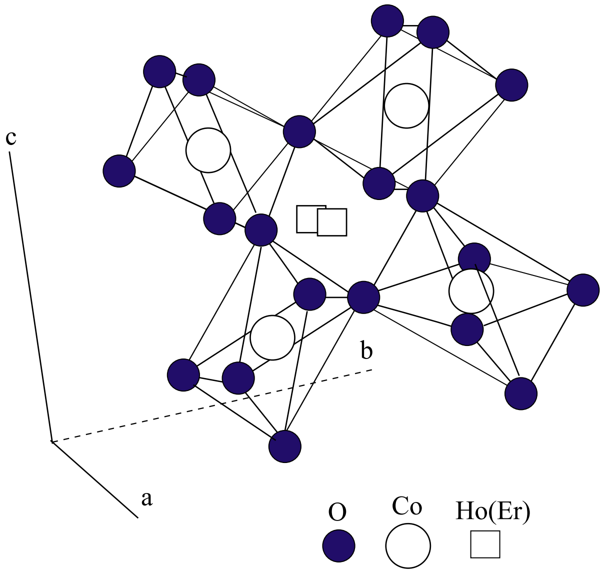

FIG. 2. Orthorhombically distorted polyhedron of holmium-doped cobalt perovskite.[11]

The least studied perovskite compounds are cobaltites with the composition $\mathrm{Re}_{1-x}\mathrm{Sr}_x\mathrm{CoO}_{3-\delta}$ with $\mathrm{Re}=\mathrm{Ho}$, Er (denoted below simply as HSCO, ESCO) as the doping additions. The use of Ho and Er as the dopants is interesting because such doping permits analyzing the particulars of the electronic correlation in systems with mixed valence with sign changes of the magnetocrystallographic anisotropy and magnetostriction, observed on going from Ho to Er. The latter is due to the fact that doping of cobalt oxides with the indicated *f* magnets results in the appearance of high energies of magnetocrystallographic anisotropy and magnetostriction, which are associated with large orbital magnetic moments in these magnets as compared with the one or two orders of magnitude smaller magnetic moments of spin-orbit nature in a *d* metal with frozen orbital moments.[8] In addition, in contrast to most perovskites with crystal structure close to cubic (manganite series), the crystal structure of cobaltites with $\mathrm{Re}=\mathrm{Ho}$, Er is subjected to very marked polyhedral distortions.

The particulars of the magnetic anisotropy which is associated with Er and Ho made it possible to count on the appearance in the cobaltites HSCO and ESCO of atypical conducting properties which motivated us to study in the present work, specifically, the transport properties of erbium cobaltites. This is first such study performed in a wide dopant concentration range $(0.99>x>0.25)$ and in combination with temperature, magnetic-field, and electric properties. In a previous work we studied the related HSCO ceramic composition.[9]

II. MATERIAL STRUCTURE. SAMPLES AND MEASUREMENT PROCEDURE

The ceramic material ESCO was synthesized by the standard three-phase technology.[10] Our x-ray diffraction studies, just as the previous structural studies of the HSCO ceramic,[11] confirmed the presence of polyhedral distortions of the cubic lattice that result in the formation of an orthorhombically distorted perovskite structure of the type *Pbnm* (GdFeO_3 prototype, Fig. 2). The basic crystallographic unit, which is the octahedron CoO_6, is turned in the *ab* plane and makes an angle with the *c* axis. In contrast to, say, LaCoO_3 the presence in the perovskite structure of rare-earth cations Er and Ho with a shorter ionic radius has a direct consequence larger deviations of the structure from undeformed cubic perovskite, such as bending of the Co–O–Co bonds by angles to 28° and shortening of the Co–O bond length induced by the lower chemical pressure.[12] As a result, according to L(S)DA band calculations,[13] the energy splitting of the crystal field $\Delta_{cf}=t_{2g}-e_g$ in cobaltites with Er and Ho is greatly increased because of preferred hybridization of the O-2*p* and Co-3*d* orbitals and the e_g band becomes narrower. Thus one could expect that the electric and transport properties of four-component compounds based on cobalt oxide with Er, just as with HO, will differ from the known properties of perovskites with other rare-earth dopants, which will give new information on the particulars of electron correlation in mixed systems.

The samples in the form of rectangular parallelepipeds were cut out with dimensions close to $0.25\times0.55\times2.5$ cm. The contact areas under the current and potential probes were deposited by ultrasonic soldering of ultrapure indium. A four-probe method with a constant stabilized current was used to perform the voltage measurements. The temperature was measured with a TP 018-03 platinum thermometer, which below 13 K was additionally calibrated at the superconducting transition temperature in lead and at liquid-helium temperature. The quality of temperature stabilization was the main determinant of the total measurement error, which in no case exceeded 10%, at “liquid helium-liquid nitrogen” and “liquid nitrogen-room temperature” intermediate temperatures.

III. RESULTS AND DISCUSSION

A. Nonlinear electric resistance in weak electric fields

Figure 3 displays the family of curves $\rho(I)$—nonlinear curves of the resistivity, normalized to the value $\rho_{T_r}(1\ \mathrm{mA})$, for samples with different dopant concentrations versus the

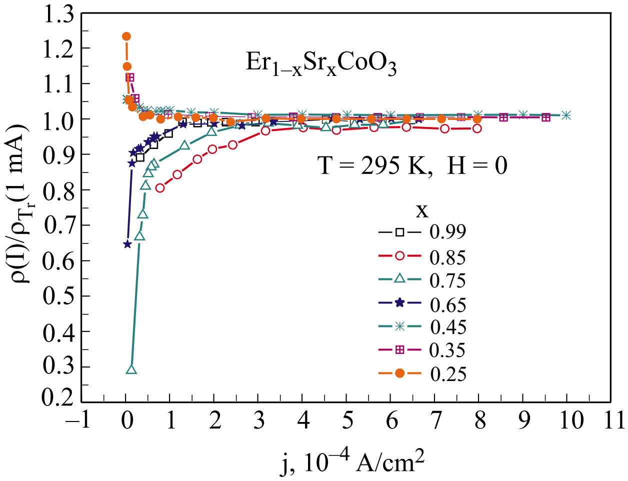

FIG. 3. Current-induced jumps of the resistance at the threshold of percolation conduction in ESCO sample with different degrees of doping at room temperature (the half-sums of the currents flowing in two directions are plotted along the *x* axis).

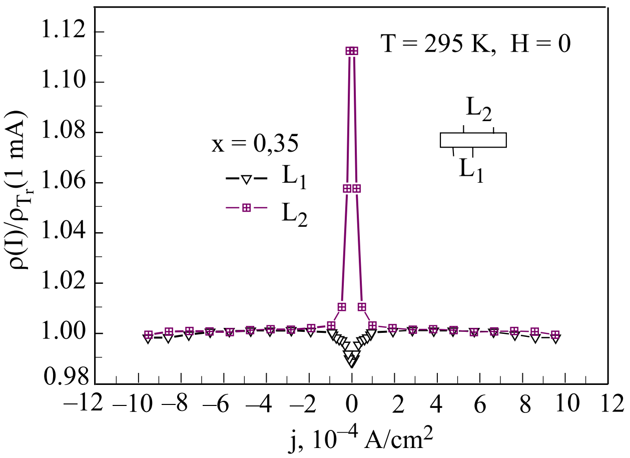

FIG. 5. Resistance jumps with different sign at the threshold of percolation conduction in different locations of one and the sample. Inset: position of the potential probes $L_1 \neq L_2$.

transport current at room temperature (T_r) and exhibiting resistance jumps in a, generally speaking, random direction.

The curves were constructed according to the data obtained from measurements of the current-voltage characteristics *U-I* for two directions of the current *I*:

$$\rho(I)/\rho(1\ \text{mA}) \equiv [U/I](I)/[U/I](1\ \text{mA}).$$

In Fig. 4 the functions $\rho(I)/\rho_{\max}$ (left-hand axis) together with the curves $E(I)$ (right-hand axis) are plotted for both measured directions of the current for two samples ($x=0.35$ and 0.65). Figure 5 illustrates for a sample with $x=0.35$ the change of the direction of the resistance jump in the function $\rho(I)/\rho_{\max}$ with a change in position of the potential probes on one and the same sample.

Figure 6 shows the current dependences of the unnormalized resistivity, averaged over two directions of the current, measured for samples with different values of *x* at liquid-nitrogen temperature (T_N), which show the universal (ordered) direction of the resistance jumps. The curves are symmetric for both current directions and similar in form to the average curves, just as the curves in Fig. 3 (compare Figs. 4 and 5), for room temperature. The peak (i.e. direction of the resistance jump) in the curve measured at the position of the probes L_1 at T_r (Fig. 5) changes sign at T_{N} (the curve for $x=0.35$ in Fig. 6 was measured on the same probes L_1).

For the four-contact measurements the "probe-sample" characteristics of the contacts do not enter in the result of the voltage measurement, in contrast to the case of two-contact measurements where the appearance of the observed nonlinear resistance jumps could be due to, for example, Schottky barriers. In addition, we studied the nonlinearities for samples with dimensions and in a current range such that there was no Joule heating impeding the separation of the characteristic nonlinear effects from secondary ones: *as current increases, the nonlinearities do not become stronger but rather vanish*, and subsequently the Ohm's linear law is observed in a reasonable interval of currents.

In summary, the nonlinear resistance jumps, which are symmetric relative to opposite directions of the current, in the curves presented in Figs. 3–6 are internal characteristics of the materials studied and are a manifestation of crossover between the regimes of non-ohmic (for weak currents) and ohmic (for currents above a threshold value) conductivity. This value of the current corresponds to an *x*-dependent threshold value of the electrostatic field strength (referred to below as the "breakdown field"). The presence of a voltage threshold for the conduction onset obviously attests, in the

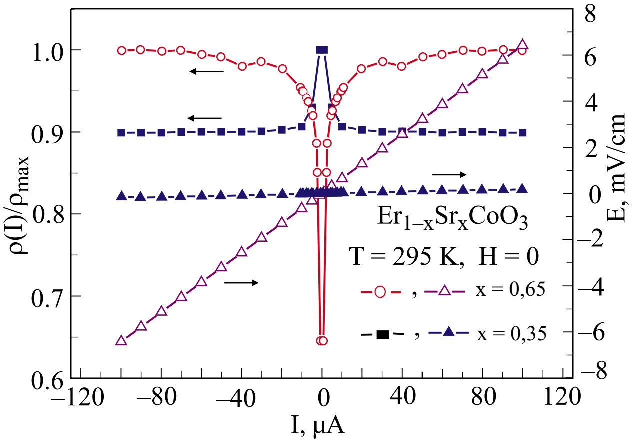

FIG. 4. Current-induced resistance jumps at the threshold of percolation conduction of two samples in both current directions together with the current/voltage curves.

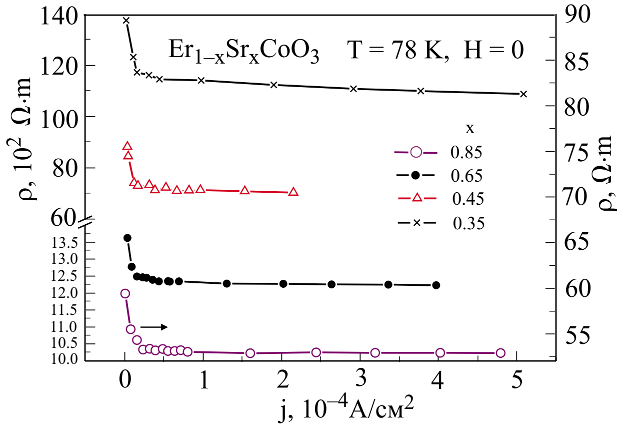

FIG. 6. Current-induced resistance jumps on the threshold of percolation conduction at temperature T_{N} for different samples.

first place, that percolation transport occurs in ceramic samples possessing a cluster structure and, in the second place, that the ohmic regime is realized beyond the percolation threshold, i.e. for electric fields much stronger than the breakdown field due to the height of the tunneling barrier at the boundary between clusters.

It goes without saying that the transition from the prethreshold "insulating" state to any type of conduction state, including percolation, must always be accompanied by a conduction jump in a universal direction (from smaller to higher values) in the case of homogeneous samples or cluster samples with the same (single-phase) character of conduction. Consequently, the observed sign change of the jump in different samples at T_r (Fig. 3–5) and at the transition from T_r to T_{N} in some samples (Figs. 3 and 5) conclusively attests that in the case of percolation conductivity in our samples the clusters are not single-phase with respect to the electronic characteristics. The data in Figs. 5 and 6 are the most eloquent evidence of the latter. The observed reversal of the jump direction with a change in the measurement positions (different pairs of potential probes) in one and the same sample (Fig. 5) and for measurements on the same pair of probes of the same sample with $T_r \to T_{\mathrm{N}}$ (Fig. 6) under conditions of percolation conduction is possible only in the presence of several phases with different conduction mechanisms, i.e. for mixed conduction even in the presence of identical clusters.

We note that conduction nonlinearities such and other types induced by the measuring current have also been observed in other perovskite materials.[9,14–17] In this connection such nonlinear effects are being widely studied, since it has become obvious that the conductivity of physically nonuniform systems is entirely determined by the competition between the activation and exchange mechanisms for percolation electron transport with strong correlation of the behavior of the electrons, so that such effects can carry important information about the nature of such mechanisms.

Returning to the concept of mixed conduction, we shall use, for example, the well-known representatives of two physically substantiated phases of the system $(\mathrm{Er}^{3+}_{1-x}\mathrm{Sr}^{2+}_{x}) \times (\mathrm{Co}^{3+}_{1-x}\mathrm{Co}^{4+}_{x})\mathrm{O}_3$. One is the ECO matrix with a hoping mechanism of conduction (for example, Mott conduction[18]), σ_s, and the other is the SCO sublattice whose conductivity, σ_F, is due to theh double-exchange mechanism.[1] Then the total conductivity σ_Σ of the system can be written in the form

$$\sigma_\Sigma = \sigma_s + \sigma_F = \sigma_s\left(1 + \frac{\sigma_F}{\sigma_s}\right);$$

$$\sigma_s \sim \sigma_F \text{ at } T \sim T_r. \tag{1}$$

It is reasonable to suppose that consecutive changes of the dopant content x in systems with double exchange should, in general, cause the ratio σ_F/σ_s to vary monotonically. Then a random change in our samples of the direction of a resistance jump, calculated from the sample-averaged voltage and associated with electric breakdown or an insulator-metal transition, can be due to only the percolation character of transport at the percolation threshold. Indeed, the expression (1) shows that the measured value of the resistance of the sample beyond the percolation threshold should be

$$R_\Sigma = R_F\left[1 + \frac{R_s}{R_F}\right]^{-1}, \tag{2}$$

where $R_i = \sigma_i^{-1}(x)K$; $i = \Sigma$, F, or s; K is the average geometric parameter "length/cross section" of the part of the sample between the potential probes (for $i = \Sigma$) or the geometric parameter of the percolation paths in all other cases. The resistance jumps in Figs. 3–6 are the quantities $\Delta R = R_0 - R_\Sigma$, where R_0 is the resistance measured before the percolation threshold on the bottom edge of the current interval and lies, together with R_Σ, in the interval $[R_F, R_s]$.

It is evident from Eq. (2) that in this case the sign of ΔR can change from one sample to another with different dopant concentrations and random geometric parameters of the percolation paths, as is observed experimentally (Figs. 3–5). In systems such as ESCO, which at room temperatures are paramagnetic and charge-disordered (most hole-doped narrow-band perovskites), the conditions for observing such nonlinear effects must be very favorable.

A completely different situation should occur at low temperatures, where σ_{ECO} is *always* much less than σ_{SCO}, so that $R_\Sigma \approx R_F$ on most of the interval $0 < x < 1$ and, evidently, in a wide range of values of K, though the character of the conduction remains mixed (see below). In this case the jump in the total resistance of the sample from the state of the insulator to the conducting (ohmic) value will always have a universal sign, $\Delta R = R_0 - R_\Sigma > 0$, as is observed at T_{N} for samples with the compositions indicated in Fig. 6.

Additional arguments supporting what has been said above give the concentration dependences, presented in Fig. 7, of the breakdown field strength at the percolation threshold. As the concentration parameter x is changed in succession, the breakdown fields at T_r vary nonmonotonically and they are several orders of magnitude weaker than at T_N for one and same samples. At liquid-nitrogen temperatures the breakdown field is an evenly varying function of x. A feature common to both curves is that the breakdown field decreases with increasing concentration of divalent strontium. This property, which has not been observed before and its observation is reported for the first time, apparently attests that as the Sr concentration increases, the energy required for the double-exchange mechanism and charge ordering to come into play, raising the conduction to ohmic, decreases.

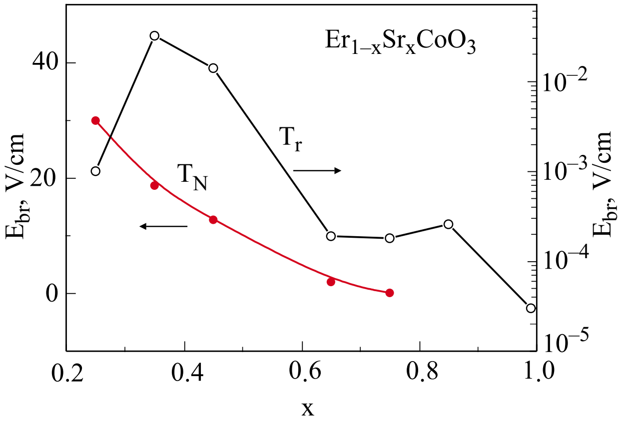

FIG. 7. Breakdown electric field at the percolation threshold as a function of the doping level of the ESCO system at two temperatures.

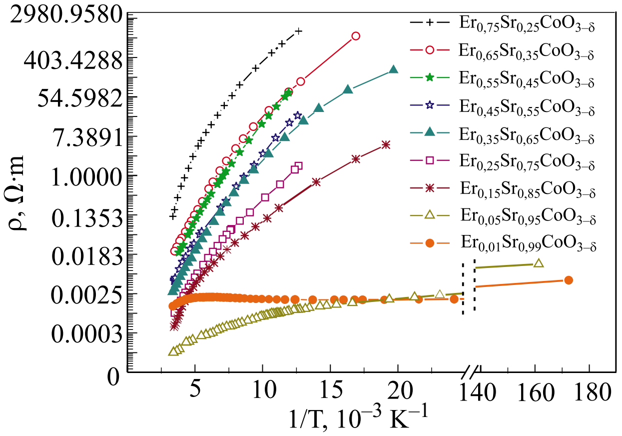

FIG. 8. Temperature dependences of the resistivity of ESCO samples in a wide range of Er and Sr concentrations.

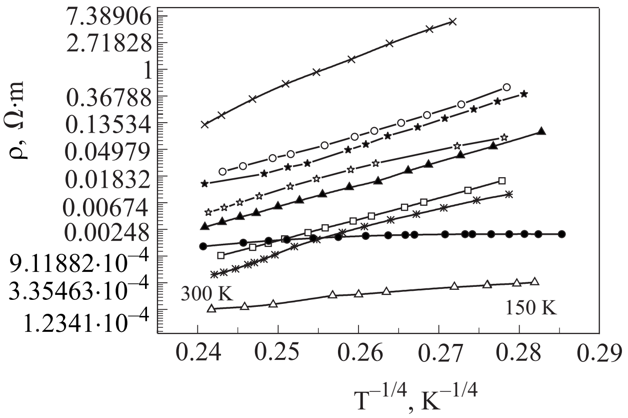

FIG. 9. High-temperature (T_r) behavior of the curves shown in Fig. 8, in thermally active Mott conductivity coordinates.

We believe that the anomalous effects such as the meal-insulator transition at the percolation threshold which manifest at low values of the bias current can be used to identify the charge-ordered state in the samples with ceramic structure.

IV. OHMIC CONDUCTIVITY ABOVE THE PERCOLATION THRESHOLD

Figure 8 displays on a logarithmic scale a family of curves of the resistivity of samples of the compound ESCO versus the reciprocal of the temperature in a wide range of values of the concentration parameter x.

The measurements were performed in the ohmic conduction region, i.e. at currents of at least 1 mA and no higher than the currents at which the conductivity becomes nonlinear because of Joule heating ($>30-50$ mA). Since the low-temperature interval on the inverse temperature scale occupies the larger portion of the X axis, the form of the curves on the scale chosen ($T<50$ K) gives an idea of the low-temperature behavior of the ohmic conductivity. As one can see, it is strongly nonlinear and closely related with the concentration of divalent Sr. As in other cobaltites,[9] the behavior of the conductivity of our samples does not correspond to that of a single-phase system, specifically, it is not described by an Arrhenius function for a purely semiconductor system.

We arrive at the same conclusion by analyzing the behavior of the same curves at temperatures close to room temperature (T_r). The curves in this region are presented in Fig. 9 in the coordinates of the function $\rho_0 \exp(AT^{-1/4})$, which describes activation "Mott" conductivity.[18] Evidently, even here the behavior of the conductivity as a function of temperature depends strongly and likewise nonmonotonically on the concentration of the dopant cations. Just as for low temperatures, the conductivity cannot be described by only *one* universal function, for example, only by an activation (hopping) type function; this likewise attests that the system is heterophase and that several types of exchange coupling clearly compete with one another, one being indirect ferromagnetic coupling via the conduction electrons, known as double exchange.

It follows from the curves in Figs. 8 and 9 that the optimal conditions for coupling of this type to manifest are realized in the concentration range $0.85<x<0.99$, where the monotonic variation of the conductivity as a function of x is interrupted and the resistivity reaches its minimum value (at $x=0.95$ for the chosen step of variation of x). In this concentration range the conductivity is so far from the semiconductor value that it can be measured in a wide temperature range right up to near-liquid-helium temperatures (down to 6 K), while for all other concentrations it can be measured at temperatures no lower than 50 K. It is evident from Fig. 10, where the corresponding curves are presented, that at the upper limit of the indicated concentration range the temperature dependence of the conductivity $\sigma(1/T)$ becomes nonmonotonic: as temperature decreases, the conductivity passes through a minimum at $T\approx150$ K and through a maximum at $T\approx50$ K. In this connection it can be supposed that in the x range under discussion, and in any case at low temperatures ($T<50$ K), with a low-spin state of Co such anomalous behavior of the conductivity, indicating the presence of a metal-insulator transition, should be related with a very strong role of the double-exchange mechanism, which competes with the direct antiferromagnetic exchange coupling between the magnetic moments of the d orbitals of cobalt ions.

If this is so, then the mixed conductivity σ_Σ of the system as the conductivity of a two-phase structure $(Er^{3+}_{1-x}Sr^{2+}_x)$ $\times(Co^{3+}_{1-x}Co^{4+}_x)O_3$, represented, just as in the preceding section, as a sum of activation conductivity of a semiconductor

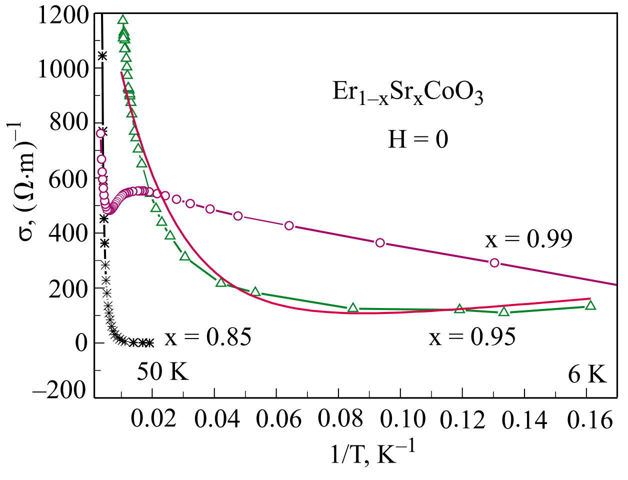

FIG. 10. Temperature behavior of the conductivity of the ESCO system in the concentration range $0.99\geqslant x\geqslant0.85$.

matrix (band-gap semiconductor), σ_s, and a ferromagnetic component, σ_F, due to the double exchange of conduction electrons between heterovalent Co ions, aligning the spins parallel to one another, can have the form

$$\sigma_\Sigma = \sigma_s + \sigma_F = \sigma_{(T_r)} \exp(-\Delta/T) + (\alpha e^2/ah)(T_C/T), \qquad (3)$$

where $\alpha = |\mathrm{Co}^{4+}|/|\mathrm{Co}^{3+}|$ is the fraction of Co^{4+} ions, T_C is the Curie temperature, a is the lattice parameter, and h is Planck's constant. The expression describes quite well the temperature dependence of the conductivity below 50 K for concentrations where double exchange is strong and a metal-insulator transition occurs (Figs. 8 and 10).

Figure 10 shows the experimental values of the conductivity as a function of the inverse temperature for concentration $0.85 \leqslant x \leqslant 0.99$ together with the solid curves describing the experimental data in accordance with the expression (3). The lattice constant $a = 5.142$ Å;[11] the values of the adjustable parameters are as follows: $T_C \approx 160$ K (see below); $\Delta \simeq 100$ K ($x = 0.99$) and $\simeq 50$ K ($x = 0.95$); $\simeq_{(T_\tau)} \simeq 675$ $(\Omega \cdot \mathrm{m})^{-1}$ ($x = 0.99$) and $1600 (\Omega \cdot \mathrm{m})^{-1}$ ($x = 0.95$); .$(\alpha e^2/ah) T_C \simeq 100$ K/$(\Omega \cdot \mathrm{m})$ ($x = 0.99$) and $\simeq 1000$ K/$(\Omega \cdot \mathrm{m})$ ($x = 0.95$). Hence it follows that the fraction of the ions Co^{4+} participating in double exchange by delocalized electrons with Co^{3+} ions is, in order of magnitude, $\alpha \sim 10^{-4} - 10^{-5}$. Comparing the ratio σ_s/σ_F at the limits of the temperature interval for the curves studied, we can verify that a metal-insulator phase transition occurs in the x range indicated:

$$\left.\frac{\sigma_s}{\sigma_F}\right|_{x=0.99} \approx \begin{cases} 45(50\ \mathrm{K}) > 1 \\ 10^{-6}(6\ \mathrm{K}) < 1 \end{cases} ;$$

$$\left.\frac{\sigma_s}{\sigma_F}\right|_{x=0.95} \approx \begin{cases} 30(50\ \mathrm{K}) > 1 \\ 12 \cdot 10^{-3}(6\ \mathrm{K}) < 1 \end{cases} .$$

The relations obtained clearly support the simultaneous presence in this system, just as in other perovskites, of antiferromagnetic (AFM) and ferromagnetic (FM) phases for all dopant concentrations; in addition, metallization as a reflection of the growing contribution of the FM phase, which lowers the energy of the system, is the result of self-consistent, free-carrier induced restructuring of the corresponding spin configurations AFM→FM.

V. MAGNETORESISTIVE EFFECT

In contrast to, for example, narrow-gap, hole-doped, four-component perovskite structures such as lanthanum manganites, the ESCO system which we studied with a smaller width of the e_g multiplet of the d band[13,19] left little hope for the appearance of a prominent magnetoresistive effect (MR). However, just as for the system HSCO,[9] this effect, though not "colossal," still can reach tens of percent in individual cases, as is evident from the data presented in Fig. 11. It follows from this figure that, first and foremost, there are two characteristic concentration ranges where the magnetoresistive effect is strong. These are the region near $x \approx 0.5$, which in the literature is called the "half-metal" region, and the region $x > 0.8$ where, as we saw above (Fig. 10), the most radical changes of the temperature behavior of the conductivity of the samples in the absence of a magnetic field are observed. The next important feature of the concentration dependences of MR presented in Fig. 11 is the sign change of MR at a transition from the temperatures T_r to T_N for $x > 0.8$. Since in "dirty" oxides, which our samples are, the dynamic properties of the carriers do not manifest for all practical purposes, the MR effects observed in perovskites should reflect phenomena directly associated with the correlation of the electronic states as a result of doping, temperature change, or application of a magnetic field, which set one or another configuration of the magnetic moments of the ions (four basic types of magnetic ordering in the basal planes of the lattices are generally recognized; Goodenough was the first one to study them[20]).

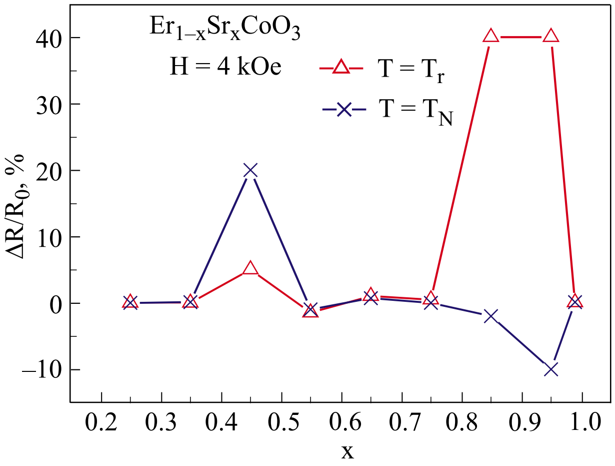

FIG. 11. Magnetoresistance $\Delta R/R_0 = [(R_H/R_0) - 1]$ versus the concentration of nonmagnetic Sr in the concentration interval $0.99 \geqslant x \geqslant 0.25$ in magnetic field 4 kOe at two temperatures.

It is reasonable to assume on the basis of our data that MR becomes appreciable ($>5\%$) in ESCO at concentrations for which the magnetic order undergoes critical changes and it becomes very sensitive to external factors, specifically, the application of very weak magnetic fields (we called attention to this in Ref. 9, where we studied the HSCO system). This is illustrated well in Fig. 12, which shows the dependence of MR for a "half metal" ($x = 0.45$) on magnetic fields no greater than 4 kOe. Comparing the MR behavior in two temperature ranges, T_r (bottom curves) and T_N (top curves), we

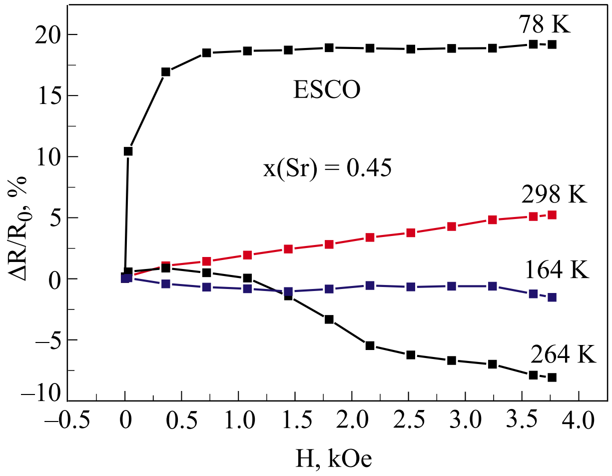

FIG. 12. Magnetoresistance of an ESCO sample with concentration of nonmagnetic Sr $x = 0.45$ versus the magnetic field.

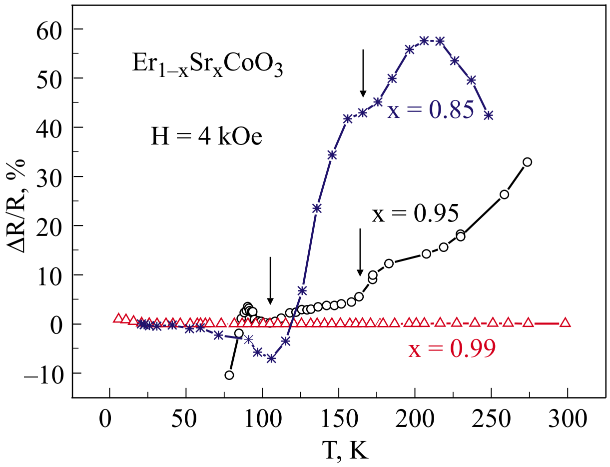

FIG. 13. Temperature dependence of the magnetoresistance $\Delta R/R_0 = [(R_H/R_0)-1]$ in the concentration interval of nonmagnetic Sr $0.99 \geqslant x \geqslant 0.85$ in magnetic field 4 kOe.

can see that for T_N the magnetic field dependence for the composition with the indicated value x has a practically “switching” character: when a field of about 1 kOe is applied the conductivity drops by almost 17% and then remains such at least to 4 kOe, while near T_r it varies smoothly as a function of H in 5–7% a range with different signs. It is clear that such a difference in the behavior of the magnetoresistive effect is possible if the character of the magnetic ordering of the structures near T_r and T_N is radically different. The same conclusion also follows from the concentration dependences of MR in Fig. 11.

The most plausible supposition is that a phase transition of the type paramagnet ↔ charge-ordered antiferromagnet ↔ ferromagnet with ordering temperature $T_{co} \approx T_C \approx 160$ K, as estimated from the position of the top kink in the MR(T) curves for other values of x (Fig. 13), occurs in the system of ions Co^{3+}/Co^{4+} in the interval T_r-T_N. This supposition is also supported by the fact that the highest value of the MR ($\approx 60\%$) in our experiment with $H=4$ kOe is attained precisely in samples with $x=0.85$ from the interval of dopant concentrations where in the absence of a magnetic field the conductivity changes radically on transitioning from $x=0.85$ to $x=0.99$ in the direction of higher values at temperatures below 100 K (see Fig. 10). Thus it can be supposed that the latter effect is associated with an AFM↔FM type phase transition (indicated approximately in Fig. 13 by the bottom arrow on the left-hand side).

VI. CONCLUSION

The temperature and concentration dependences of the electric resistance of ceramic samples $Er_{1-x}Sr_xCoO_{3-\delta}$ were studied from room to liquid-helium temperatures for erbium concentrations $0.01 < 1-x < 0.75$ and in magnetic fields to 4 kOe applied perpendicular to the direction of the transport current.

Current-induced nonlinearities of percolation transport (ER), which are characteristic for a metal-insulator transition, were found for weak currents in the absence of magnetic fields. Behavior such as a decrease of the breakdown field with increasing concentration of divalent strontium and charge-ordering effects with decreasing temperature have been observed for the first time. It was proposed that as the Sr concentration increases, the probability of tunneling of the carriers on the basis of the mechanism of double exchange between heterovalent cobalt ions increases also, as a result of which ohmic values of the conductivity are reached.

An anomalous increase of the conductivity and a strong magnetoresistive effect were observed in a narrow range of Er and Sr concentrations, narrower and more shifted in the direction of the metallic phase than in lanthanum manganites. Analysis of the data attests to the presence in ESCO of a very narrow hybridized $3d/e_g$ band, supposedly due to orthorhombic polyhedral distortions of the lattice because of the chemical pressure due to the small radius of the erbium ion. The behavior of the conductivity and MR are explained, just as nonlinear ER effects, from a unified viewpoint—magnetostructural phase transitions, induced by a corresponding concentration of dopants, temperature, and magnetic field, as well as the presence of spin-dependent contribution to the electron-correlation mechanism associated with double exchange of delocalized electrons. This contribution to the conductivity of the system below 50 K was evaluated.

[a] Email: chiang@ilt.kharkov.ua

---

[1] C. Zener, Phys. Rev. **82**, 403 (1951).
[2] S. Jin, T. H. Tiefel, M. McCormack, P. A. Fastnacht, R. Ramesh, and L. H. Chen, Science **264**, 413 (1994).
[3] A. Georges, G. Kotliar, W. Krauth, and M. J. Rozenberg, Rev. Mod. Phys. **68**, 13 (1996).
[4] V. M. Loktev, Yu. G. Pogorelov, Fiz. Nizk. Temp. **26**, 231 (2000) [Low Temp. Phys. **26**, 171 (2000)].
[5] Yu. A. Izyumov and Yu. N. Skryabin, Usp. Fiz. Nauk **171**, 121 (2001).
[6] M. N. Baibich, J. M. Broto, A. Pert, F. Nguyen Van Dau, F. Petroff, P. Eitenne, G. Creuzet, A. Friederich, and J. Chazelas, Phys. Rev. Lett. **61**, 2472 (1988).
[7] Yu. N. Chiang, O. G. Shevchenko, and R. N. Kolenov, Fiz. Nizk. Temp. **31**, 1117 (2005) [Low Temp. Phys. **31**, 852 (2005)].
[8] Yu. P. Irkhin, Usp. Fiz. Nauk **154**, 321 (1988).
[9] Yu. N. Chiang, V. F. Khirnyĭ, O. G. Shevchenko, A. A. Kozlovskiĭ, A. M. Semenov, V. M. Puzikov, and T. G. Deĭneka, Fiz. Nizk. Temp. **34**, 1197 (2008) [Low Temp. Phys. **34**, 947 (2008)].
[10] A. A. Kozlovs'kiĭ, V. P. Khirniĭ, and T. G. Deĭneka, O. V. Semenov, and V. M. Puzikov, Nanosistemi, nanomateriali, nanotekhnologii **5**, 609 (2007).
[11] X. Liu and C. T. Prewitt, J. Phys. Chem. Solids **52**, 441 (1991).
[12] P. O. Radaelli and S.-W. Cheong, Phys. Rev. B **66**, 094408 (2002).
[13] I. A. Nekrasov, S. V. Streltsov, M. A. Korotin, and V. I. Anisimov, Phys. Rev. B **68**, 235113 (2003).
[14] A. Guha, A. K. Raychaudhuri, A. R. Raju, and C. N. R. Rao, Phys. Rev. B **62**, 5320 (2000).
[15] Y. Yuzhelevski, V. Markovich, V. Dikovsky, E. Rozenberg, G. Gorodetsky, G. Jung, D. A. Shulyatev, and Y. M. Mukovskii, Phys. Rev. B **64**, 224428 (2001).
[16] N. Biskup, A. de Andres, I. M. Ochando, and M. T. Casais, Phys. Rev. B **73**, 184404 (2006).
[17] K. Bajaj, J. Jesudasan, V. Bagwe, D. C. Kothari, and P. Ray Chaudhuri, J. Phys.: Condens. Matter **19**, 382202 (2007).
[18] N. F. Mott, *Metal—Insulator Transitions*, Taylor and Francis, London (1990).
[19] A. Abraham and B. Bleany, *Electron Paramagnetic Resonance of Transition Metals*, Clarendon Press, Oxford (1970).

Translated by M. E. Alferieff